Alexandria Engineering Journal (2022) 61, 11301–11312

HOSTED BY

Alexandria University

Alexandria Engineering Journal

www.elsevier.com/locate/aej
www.sciencedirect.com

Dynamical behavior of a fractional-order Hantavirus infection model incorporating harvesting

Mahmoud Moustafa [a,c], Farah Aini Abdullah [b,*], Sharidan Shafie [a,*], Zuhaila Ismail [a]

[a] Department of Mathematical Sciences, Faculty of Science, Universiti Teknologi Malaysia, Malaysia
[b] School of Mathematical Sciences, Universiti Sains Malaysia, Pulau Pinang, Malaysia
[c] Department of Cyber Security, College of Engineering & Information Technology, Onaizah Colleges, Onaizah P.O. Box 5371, Saudi Arabia

Received 4 March 2022; revised 21 April 2022; accepted 7 May 2022
Available online 19 May 2022

KEYWORDS

Hantavirus;
Fractional order;
Stability;
Sotomayor's theorem;
Numerical simulation

Abstract In this paper, a fractional-order Hantavirus infection model incorporating harvesting is formulated and investigated. The populations are divided into susceptible mice, infected mice and alien species. Mathematical analysis and numerical simulations are performed to clarify the characteristics of the proposed fractional-order Hantavirus infection model. The existence, uniqueness, non-negativity and boundedness of the solutions are examined. The local stability of the equilibrium points of the fractional-order model is studied. The mathematical proof of the existence of transcritical bifurcation is given by using Sotomayor's theorem. The theoretical findings are illustrated by numerical simulations. The impact of fractional-order, competitive effect of alien species on mice, competitive effect of mice on alien species, carrying capacity and harvesting efforts on the stability of the Hantavirus infection model are studied. The basin of attraction regions is also illustrated.

1. Introduction

Hantavirus infection is a viral disease that is spread from mice to people. The virus can cause severe infections of the lungs [1]. The dynamics of Hantavirus epidemics involve multiple phases, including environmental drivers that influence infectious diseases and transmission in the animal reservoir. By further studying the transmission dynamics of Hantavirus, critical insight can be obtained into the ecology of Hantavirus [2]. Hantavirus infection can occur in a system consisting of the host species and a non-host competitor species which competes for resources. The competition may lead to a reduction or complete elimination of the prevalence of Hantavirus infection [3]. A Hantavirus infection model can be used to make predictions about the behavior of interacting populations. Some studies about the simulations in the mathematical modeling of the spread of the Hantavirus include [4–9]. Incorporating

* Corresponding authors.
E-mail addresses: mahmoudmoustafa949@gmail.com (M. Moustafa), farahaini@usm.my (F.A. Abdullah), sharidan@utm.my (S. Shafie), zuhaila@utm.my (Z. Ismail).

Peer review under responsibility of Faculty of Engineering, Alexandria University.

https://doi.org/10.1016/j.aej.2022.05.004

harvesting to Hantavirus model is expected to provide a more realistic model since for a number of mice some form of harvesting in the ecosystem is known to occur.

A Hantavirus infection model, which employs a three-species of non-linear ordinary differential equations introduced in [10] is considered in this paper. The dynamics of the population density of susceptible mice (x), infected mice (y) and alien species $(z)$are as follows

$$\begin{aligned}
\tfrac{dx}{dt} &= \hat{b}(x+y) - \hat{c}x - \tfrac{\hat{b}x}{\hat{k}}(x+y+\hat{\alpha}z) - \hat{a}xy - \widehat{H}x,\ x(0) = x_0,\\
\tfrac{dy}{dt} &= -\hat{c}y - \tfrac{\hat{b}y}{\hat{k}}(x+y+\hat{\alpha}z) + \hat{a}xy - \widehat{H}y,\ y(0) = y_0,\\
\tfrac{dz}{dt} &= \left(\hat{\beta} - \hat{\gamma}\right)z - \tfrac{\hat{\beta}z}{\hat{k}}(z + \hat{\epsilon}(x+y)),\ z(0) = z_0.
\end{aligned} \tag{1}$$

All the parameters are non-negative for all time $t \geqslant 0$ and are explained in Table 1. It is assumed that the alien species grow logistically in the absence of mice. It is also assumed that the Hantavirus does not harm an infected mouse and the disease is not transmitted by an infected mouse to a newborn (no vertical transmission).

Fractional-order differential equations as a basis of mathematical models have been applied in ecological models [11–17], epidemic models [18–28], eco-epidemic models [29,30] and chaotic models [31] to investigate the underlying dynamics of the models. The fractional-order derivative is a non-local operator and related to models with memory. The fractional derivative of a biological process at a one-point depends on all of the information and behavior of the model in all previous moments, while the classical derivative in one point is affected only from the information in the local neighborhood of that point [32]. The presence of fractional-order derivative in the Hantavirus infection models generalizes the results obtained in case of the standard derivative in that the memory effects offered by fractional-order derivative can measure the caution of the populations [33]. These features enables fractional-order differential equations to model the phenomena having non-Markovian behavior (where the state of the model at each time depends on the previous history of the model) [34]. Thus, the fractional-order derivative may be more suitable for the Hantavirus infection model with harvesting that is dependent on past history [35]. Additionally, the fractional-order model is more realistic to experimental datasets than its integer-order counterpart model [36]. Hence, the dynamics of the relations between susceptible mice, infected mice and alien species incorporating harvesting can be more accurately described by fractional-order models. In addition, the stability region of the Hantavirus infection model can be extended by the fractional-order derivative.

Table 1 Biological description of parameters used.

Symbol	Description
$\hat{k}$	Carrying capacity
$\hat{c}$	Natural death rate of mice
$\hat{b}$	Birth rate of mice
$\hat{a}$	Transmission rate of Hantavirus
$\widehat{H}$	Harvesting efforts
$\hat{\beta}$	Birth rate of alien species
$\hat{\gamma}$	Death rate of alien species
$\hat{\alpha}$	Competitive effect of alien species on mice
$\hat{\epsilon}$	Competitive effect of mice on alien species.

In this study, a new model can be constructed by incorporating the Caputo fractional derivative of order $q({}^cD^q)$ into the counterpart integer order model (1) as follows:

$$\begin{aligned}
{}^cD^q x(t) &= \hat{b}(x+y) - \hat{c}x - \tfrac{\hat{b}x}{\hat{k}}(x+y+\hat{\alpha}z) - \hat{a}xy - \widehat{H}x,\ x(0) = x_0,\\
{}^cD^q y(t) &= -\hat{c}y - \tfrac{\hat{b}y}{\hat{k}}(x+y+\hat{\alpha}z) + \hat{a}xy - \widehat{H}y,\ y(0) = y_0,\\
{}^cD^q z(t) &= \left(\hat{\beta} - \hat{\gamma}\right)z - \tfrac{\hat{\beta}z}{\hat{k}}(z + \hat{\epsilon}(x+y)),\ z(0) = z_0,
\end{aligned} \tag{2}$$

where $q \in (0,1)$ and ${}^cD^q$ denotes Caputo differentiation [37]. The right-hand side expressions of the model (2) have a dimension $(time)^{-1}$, whereas the left-hand sides have a dimension $(time)^{-q}$. To have the dimensions match, the model (2) can be rewritten as follows:

$$\begin{aligned}
{}^cD^q x(t) &= \hat{b}^q(x+y) - \hat{c}^q x - \tfrac{\hat{b}^q x}{\hat{k}}(x+y+\hat{\alpha}z) - \hat{a}^q xy - \widehat{H}^q x,\ x(0) = x_0,\\
{}^cD^q y(t) &= -\hat{c}^q y - \tfrac{\hat{b}^q y}{\hat{k}}(x+y+\hat{\alpha}z) + \hat{a}^q xy - \widehat{H}^q y,\ y(0) = y_0,\\
{}^cD^q z(t) &= \left(\hat{\beta}^q - \hat{\gamma}^q\right)z - \tfrac{\hat{\beta}^q z}{\hat{k}}(z + \hat{\epsilon}(x+y)),\ z(0) = z_0.
\end{aligned} \tag{3}$$

For simplification, the model (3) can be redefined with the following new parameters [38]:

$$\hat{b}^q = b, \hat{k} = k, \hat{c}^q = c, \hat{\alpha} = \alpha, \hat{a}^q = a, \widehat{H}^q = H,$$
$$\hat{\beta}^q = \beta, \hat{\epsilon} = \epsilon, \text{and} \hat{\gamma}^q = \gamma.$$

Then, the model (3) becomes as follows:

$$\begin{aligned}
{}^cD^q x(t) &= b(x+y) - cx - \tfrac{bx}{k}(x+y+\alpha z) - axy - Hx,\ x(0) = x_0,\\
{}^cD^q y(t) &= -cy - \tfrac{by}{k}(x+y+\alpha z) + axy - Hy,\ y(0) = y_0,\\
{}^cD^q z(t) &= (\beta - \gamma)z - \tfrac{\beta z}{k}(z + \epsilon(x+y)),\ z(0) = z_0.
\end{aligned} \tag{4}$$

So far as we are aware, the dynamics of the proposed fractional-order Hantavirus infection model (4) has not been investigated. Therefore, this paper seeks to investigate the dynamics of the proposed fractional-order Hantavirus infection model incorporating harvesting. In order to clarify the characteristics of the proposed fractional-order Hantavirus infection model, the analysis of existence, uniqueness, non-negativity and boundedness of the solutions are examined. The contribution of this paper is to extend the classical model of the Hantavirus infection model with harvesting to a new model based on the Caputo fractional derivatives with logistic growth rate. The paper also investigates the local stability of the equilibrium points of the proposed fractional-order Hantavirus model which can be considered as the main contribution of this paper. The proof of the existence of transcritical bifurcation is also given by using Sotomayor's theorem. Some threshold parameters are obtained to determine the existence and stability conditions of equilibrium points. Numerical simulations are given to illustrate the properties of the proposed fractional-order Hantavirus model regarding fractional-order (q), competitive effect of alien species on mice (α), competitive effect of mice on alien species (ϵ), carrying capacity $(k)$and harvesting efforts (H)which is in agreement with the theoretical analysis. The basin of attraction regions is also illustrated.

The outline of this study is as follows. Sections 2–5 present the mathematical analysis of the proposed fractional-order Hantavirus model. Section 6 provides the numerical simulations. Section 7 gives the conclusion.

2. Equilibrium points

Studying equilibrium solutions is important in epidemic models because it predicts long-term behaviors of a system [39,40]. In this section, we will use the following threshold parameters.

$$\Re_0 = \frac{ak(b-\zeta)}{b^2}, \Re_1 = \frac{b\beta}{bd\alpha + \beta\zeta},$$
$$\Re_2 = \frac{bd}{\beta\epsilon(b-\zeta)} \text{and} \Re_3 = \frac{b\beta(\epsilon\alpha b + ak)}{ak(bd\alpha + \beta\zeta) + b^2\beta},$$

where, $\zeta = c + H$ and $d = \beta - \gamma$.

The fractional-order Hantavirus infection model (4) has the following six equilibrium points:

1. $E_0 = (0, 0, 0)$, which always exists.
2. $E_1 = \left(\frac{k(b-\zeta)}{b}, 0, 0\right)$, which exists if $b > \zeta$.
3. $E_2 = \left(0, 0, \frac{dk}{\beta}\right)$, which exists if $d > 0$.
4. $E_3 = \left(\frac{b}{a}, \frac{b}{a}(\Re_0 - 1), 0\right)$, which exists if $\Re_0 > 1$.
5. $E_4 = \left(\frac{k(bd\alpha+\beta\zeta)}{b\beta(\epsilon\alpha-1)}(1-\Re_1), 0, \frac{k(\beta\epsilon(b-\zeta))}{b\beta(\epsilon\alpha-1)}(1-\Re_2)\right)$,
   (a) when $\epsilon\alpha > 1, E_4$ exists if $\Re_1 < 1$ and $\Re_2 < 1$,
   (b) when $\epsilon\alpha < 1, E_4$ exists if $\Re_1 > 1$ and $\Re_2 > 1$.
6. $E_5 = \left(\frac{b}{a}, \frac{ak(bd\alpha+\beta\zeta)+b^2\beta}{ab\beta(\epsilon\alpha-1)}(1-\Re_3), \frac{k(\beta\epsilon(b-\zeta))}{b\beta(\epsilon\alpha-1)}(1-\Re_2)\right)$,
   (a) when $\epsilon\alpha > 1, E_5$ exists if $\Re_3 < 1$ and $\Re_2 < 1$,
   (b) when $\epsilon\alpha < 1, E_5$ exists if $\Re_3 > 1$ and $\Re_2 > 1$.

3. Existence and uniqueness of the solutions

The existence and uniqueness of the solutions of the fractional-order Hantavirus infection model (4) in the region $\Omega \times (0, T]$ where

$$\Omega = \{(x, y, z) \in \mathbb{R}^3 : \max(|x|, |y|, |z|) \leqslant \theta\},$$

can be studied as follows.

Theorem 1. For each $X_0 = (x_0, y_0, z_0) \in \Omega$, there exists a unique solution $X(t) \in \Omega$ of Hantavirus infection model (4) with initial condition $X_0, \forall t \geqslant 0$.

Proof. The mapping

$$W(X) = (W_1(X), W_2(X), W_3(X)),$$

is considered, where

$$\begin{aligned} W_1(X) &= b(x+y) - \zeta x - \tfrac{bx}{k}(x+y+\alpha z) - axy, \\ W_2(X) &= -\zeta y - \tfrac{by}{k}(x+y+\alpha z) + axy, \\ W_3(X) &= dz - \tfrac{\beta z}{k}(z + \epsilon(x+y)). \end{aligned} \tag{5}$$

For any $X, \overline{X} \in \Omega$, it follows from (5) that

$$\begin{aligned} \|W(X) - W(\overline{X})\| = {} & |W_1(X) - W_1(\overline{X})| + |W_2(X) - W_2(\overline{X})| + |W_3(X) - W_3(\overline{X})| \\ &= \left|b(x+y) - \zeta x - \tfrac{bx}{k}(x+y+\alpha z) - axy - b(\bar{x}+\bar{y}) + \zeta\bar{x} + \tfrac{b\bar{x}}{k}(\bar{x}+\bar{y}+\alpha\bar{z}) + a\bar{x}\bar{y}\right| \\ &+ \left|-\zeta y - \tfrac{by}{k}(x+y+\alpha z) + axy + \zeta\bar{y} + \tfrac{b\bar{y}}{k}(\bar{x}+\bar{y}+\alpha\bar{z}) - a\bar{x}\bar{y}\right| \\ &+ \left|dz - \tfrac{\beta z}{k}(z + \epsilon(x+y)) - d\bar{z} + \tfrac{\beta\bar{z}}{k}(\bar{z} + \epsilon(\bar{x}+\bar{y}))\right| \\ &\leqslant (b+\zeta)|x-\bar{x}| + (b+\zeta)|y-\bar{y}| + d|z-\bar{z}| \\ &+ \tfrac{b}{k}|x-\bar{x}||x+\bar{x}| + \tfrac{b}{k}|y-\bar{y}||y+\bar{y}| + \tfrac{\beta}{k}|z-\bar{z}||z+\bar{z}| \\ &+ \left(\tfrac{2b}{k} + 2a\right)|xy - \bar{x}y + \bar{x}y - \bar{x}\bar{y}| + \left(\tfrac{b\alpha+\epsilon\beta}{k}\right)|yz - \bar{y}z + \bar{y}z - \bar{y}\bar{z}| \\ &+ \left(\tfrac{b\alpha+\epsilon\beta}{k}\right)|xz - \bar{x}z + \bar{x}z - \bar{x}\bar{z}| \\ &\leqslant (b+\zeta)|x-\bar{x}| + (b+\zeta)|y-\bar{y}| + d|z-\bar{z}| \\ &+ \tfrac{2b\theta}{k}|x-\bar{x}| + \tfrac{2b\theta}{k}|y-\bar{y}| + \tfrac{2\beta\theta}{k}|z-\bar{z}| \\ &+ 2\left(\tfrac{b}{k}+a\right)\theta|x-\bar{x}| + 2\left(\tfrac{b}{k}+a\right)\theta|y-\bar{y}| \\ &+ \left(\tfrac{b\alpha+\epsilon\beta}{k}\right)\theta|y-\bar{y}| + \left(\tfrac{b\alpha+\epsilon\beta}{k}\right)\theta|z-\bar{z}| \\ &+ \left(\tfrac{b\alpha+\epsilon\beta}{k}\right)\theta|x-\bar{x}| + \left(\tfrac{b\alpha+\epsilon\beta}{k}\right)\theta|z-\bar{z}| \\ &\leqslant \left(b+\zeta+\tfrac{2b\theta}{k} + 2\left(\tfrac{b}{k}+a\right)\theta + \left(\tfrac{b\alpha+\epsilon\beta}{k}\right)\theta\right)|x-\bar{x}| \\ &+ \left(b+\zeta+\tfrac{2b\theta}{k} + 2\left(\tfrac{b}{k}+a\right)\theta + \left(\tfrac{b\alpha+\epsilon\beta}{k}\right)\theta\right)|y-\bar{y}| \\ &+ \left(d + \tfrac{2\beta\theta}{k} + 2\left(\tfrac{b\alpha+\epsilon\beta}{k}\right)\theta\right)|z-\bar{z}| \\ &\leqslant U\|X - \overline{X}\|, \end{aligned}$$

where

$$\begin{aligned} U = \max\Bigg\{ & b + \zeta + \frac{2b\theta}{k} + 2\left(\frac{b}{k} + a\right)\theta + \left(\frac{b\alpha+\epsilon\beta}{k}\right)\theta, d \\ & + \frac{2\beta\theta}{k} + 2\left(\frac{b\alpha+\epsilon\beta}{k}\right)\theta \Bigg\}. \end{aligned}$$

Thus, $W(X)$ satisfies the Lipschitz condition. So there exists a unique solution $X(t)$of the Hantavirus infection model (4) with initial condition $X_0 = (x_0, y_0, z_0)$. □

4. Non-negativity and boundedness of solutions

The non-negativity of the solutions of the model (4) can be given as follows From Hantavirus infection model (4), one has

$$\begin{aligned} {}^cD^q x(t)|_{x=0} &= by \geqslant 0, \\ {}^cD^q y(t)|_{y=0} &= 0, \\ {}^cD^q z(t)|_{z=0} &= 0. \end{aligned}$$

Also, the model satisfies the Lipschitz condition as stated in Theorem 1. According to Theorem 5 and Theorem 6 in [41], it can deduce that the solutions of the fractional-order Hantavirus infection model (4) are non-negative.

The following theorem investigates the boundedness of the solutions.

Theorem 2. The solutions of the fractional-order Hantavirus infection model (4) starting in $\mathbb{R}^3_+$ are bounded.

Proof. Firstly, the following function

$$M(t) = x(t) + y(t),$$

can be considered to study the boundedness of the first two equations of model (4), then one has

$$\begin{aligned} {}^cD^q M(t) &= {}^cD^q x + {}^cD^q y \\ &= bM - \zeta x - \tfrac{bx}{k}(M + \alpha z) - \zeta y - \tfrac{by}{k}(M + \alpha z) \\ &= bM - \zeta M - \tfrac{bM^2}{k} - \tfrac{b\alpha Mz}{k} \\ &\leqslant bM - \zeta M - \tfrac{bM^2}{k}, \end{aligned}$$

thus,

$$\begin{aligned} {}^{c}D^{q}M(t)+\zeta M(t) &\leqslant bM-\tfrac{bM^2}{k} \\ &\leqslant -\tfrac{b}{k}\left(M^2-kM\right) \\ &\leqslant -\tfrac{b}{k}\left(M-\tfrac{k}{2}\right)^2+\tfrac{bk}{4} \\ &\leqslant \tfrac{bk}{4}. \end{aligned}$$

In accordance with Lemma 9 in [42], one has

$$0 \leqslant M(t) \leqslant M(0)E_q(-\zeta t^q)+\frac{bk}{4}\,t^q E_{q,q+1}(-\zeta t^q),$$

By using Lemma 5 and Corollary 6 in [42], it follows that

$$0 \leqslant M(t) \leqslant \frac{bk}{4\zeta}, \text{as} t \to \infty.$$

Secondly, in order to study the boundedness of the third equation of Hantavirus infection model (4), one has

$$\begin{aligned} {}^{c}D^{q}z &= dz-\tfrac{\beta z^2}{k}-\tfrac{\beta\epsilon z(x+y)}{k} \\ &\leqslant dz-\tfrac{\beta z^2}{k}, \end{aligned}$$

then,

$$\begin{aligned} {}^{c}D^{q}z+dz &\leqslant 2dz-\tfrac{\beta z^2}{k} \\ &\leqslant -\tfrac{\beta}{k}\left(z^2-\tfrac{2dk}{\beta}z+\left(\tfrac{dk}{\beta}\right)^2\right)+\tfrac{d^2k}{\beta} \\ &\leqslant -\tfrac{\beta}{k}\left(z-\tfrac{dk}{\beta}\right)^2+\tfrac{d^2k}{\beta} \\ &\leqslant \tfrac{d^2k}{\beta}. \end{aligned}$$

In accordance with Lemma 9 in [42], one has

$$0 \leqslant z(t) \leqslant z(0)E_q(-dt^q)+\frac{d^2k}{\beta}\,t^q E_{q,q+1}(-dt^q).$$

By using Lemma 5 and Corollary 6 in [42], it follows that

$$0 \leqslant z(t) \leqslant \frac{dk}{\beta}, \text{as} t \to \infty.$$

Therefore, the solutions of Hantavirus infection model (4) starting in $\mathbb{R}^3_+$are uniformly bounded in the region M_1, where

$$M_1=\left\{(x,y,z)\in R^3_+ : x+y \leqslant \frac{bk}{4\zeta}+v \text{and} z \leqslant \frac{dk}{\beta}+v,\ v>0\right\}. \tag{6}$$

5. Local stability analysis

The local stability analysis is now studied. The Jacobian matrix of Hantavirus infection model (4) is as follows:

$$J(x,y,z)=\begin{pmatrix} -\frac{b(2x+y+\alpha z-k)+k(ay+\zeta)}{k} & b-\frac{(b+ak)x}{k} & -\frac{\alpha bx}{k} \\ (a-\frac{b}{k})y & ax-\zeta-\frac{b(x+2y+\alpha z)}{k} & -\frac{\alpha by}{k} \\ -\frac{\epsilon\beta z}{k} & -\frac{\epsilon\beta z}{k} & d-\frac{\beta(\epsilon(x+y)+2z)}{k} \end{pmatrix}. \tag{7}$$

Theorem 3. The E_0 of Hantavirus infection model (4) is locally stable if $\beta<\gamma$ and $b<\zeta$.

Proof. The Jacobian matrix (7) evaluated at the E_0 is the following

$$J(E_0)=\begin{pmatrix} b-\zeta & b & 0 \\ 0 & -\zeta & 0 \\ 0 & 0 & \beta-\gamma \end{pmatrix}. \tag{8}$$

The eigenvalues of matrix (8) are $\mu_1=\beta-\gamma, \mu_2=-\zeta$ and $\mu_3=b-\zeta$. Following the Matignon's condition [43,40], one has $|arg(\mu_2)|=\pi>\frac{q\pi}{2}$. If $\beta<\gamma$ and $b<\zeta$then, $|arg(\mu_{1,3})|=\pi>\frac{q\pi}{2}\ \forall\ q\in(0,1)$. Thus, E_0 is locally stable if $\beta<\gamma$ and $b<\zeta$. □

Theorem 4. The equilibrium point E_1 of Hantavirus infection model (4) is locally stable if $\Re_0<1$ and $\Re_2<1$.

Proof. The $J(E_1)$ is as following

$$J(E_1)=\begin{pmatrix} \zeta-b & \zeta+ak(\frac{\zeta}{b}-1) & \alpha(\zeta-b) \\ 0 & b(\Re_0-1) & 0 \\ 0 & 0 & \frac{\beta\epsilon(\zeta-b)}{b}(1-\Re_2) \end{pmatrix}. \tag{9}$$

The eigenvalues of matrix (9) are $\mu_1=\zeta-b, \mu_2=b(\Re_0-1)$ and $\mu_3=\frac{\beta\epsilon(\zeta-b)}{b}(1-\Re_2)$. Following the Matignon's condition [43,40], one has $|arg(\mu_1)|=\pi>\frac{q\pi}{2}$. If $\Re_0<1$ and $\Re_2<1$then, $|arg(\mu_{2,3})|=\pi>\frac{q\pi}{2}\ \forall\ q\in(0,1)$. Therefore, E_1 is locally stable if $\Re_0<1$ and $\Re_2<1$. □

Theorem 5. The E_2 of Hantavirus infection model (4) is locally stable if $\Re_1<1$.

Proof. The $J(E_2)$is as follows

$$J(E_2)=\begin{pmatrix} \frac{\beta\zeta+bd\alpha}{\beta}(\Re_1-1) & b & 0 \\ 0 & -\frac{bd\alpha+\beta\zeta}{\beta} & 0 \\ -\epsilon d & -\epsilon d & -d \end{pmatrix}. \tag{10}$$

The eigenvalues of matrix (10) are $\mu_1=-d, \mu_2=\frac{\beta\zeta+bd\alpha}{\beta}(\Re_1-1)$ and $\mu_3=-\frac{bd\alpha+\beta\zeta}{\beta}$. Following the Matignon's condition [43,40], one has $|arg(\mu_{1,3})|=\pi>\frac{q\pi}{2}$. If $\Re_1<1$ then, $|arg(\mu_2)|=\pi>\frac{q\pi}{2}\ \forall\ q\in(0,1)$. Therefore, E_2 is locally stable if $\Re_1<1$. □

Theorem 6. The E_3 of Hantavirus infection model (4) is locally stable if $\Re_0>1$and $\Re_2<1$.

Proof. The $J(E_3)$given by

$$J(E_3)=\begin{pmatrix} \frac{ak\zeta}{b}+b-ak-\frac{b^2}{ak} & -\frac{b^2}{ak} & -\frac{\alpha b^2}{ak} \\ (a-\frac{b}{k})(k-\frac{b}{a}-\frac{k\zeta}{b}) & \zeta+b(\frac{b}{ak}-1) & \alpha(\zeta+b(\frac{b}{ak}-1)) \\ 0 & 0 & \frac{\beta\epsilon(b-\zeta)}{b}(\Re_2-1) \end{pmatrix}. \tag{11}$$

The eigenvalues of matrix (11) are $\mu_1=\zeta-b$, $\mu_2=\frac{\beta\epsilon(b-\zeta)}{b}(\Re_2-1)$and $\mu_3=\frac{ak\zeta}{b}+b-ak$ which is equivalent to $b(1-\Re_0)$. Following the Matignon's condition [43,40], one has $|arg(\mu_1)|=\pi>\frac{q\pi}{2}$. If $\Re_2<1$ and $\Re_0>1$ then, $|arg(\mu_{2,3})|=\pi>\frac{q\pi}{2}\ \forall\ q\in(0,1)$. Therefore, E_3 is locally stable if $\Re_0>1$and $\Re_2<1$ which implies that the disease will be an endemic. □

Theorem 7. The E_4 of Hantavirus infection model (4) is locally stable if $\zeta > ax_4 - \frac{b(x_4+\alpha z_4)}{k}$and $\epsilon\alpha < 1$.

Proof. The $J(E_4)$given by

$$J(E_4) = \begin{pmatrix} -\frac{bx_4}{k} & b - \frac{(b+ak)x_4}{k} & -\frac{\alpha bx_4}{k} \\ 0 & ax_4 - \zeta - \frac{b(x_4+\alpha z_4)}{k} & 0 \\ -\frac{\epsilon\beta z_4}{k} & -\frac{\epsilon\beta z_4}{k} & -\frac{\beta z_4}{k} \end{pmatrix}. \tag{12}$$

The eigenvalues of matrix (12) are $\mu_1 = ax_4 - \zeta - \frac{b(x_4+\alpha z_4)}{k}$ and the other two eigenvalues $\mu_{2,3}$are the roots of the following equation:

$$\mu^2 + \frac{1}{k}(bx_4 + \beta z_4)\mu + \frac{b\beta x_4 z_4}{k^2}(1 - \epsilon\alpha) = 0.$$

If $\zeta > ax_4 - \frac{b(x_4+\alpha z_4)}{k}$ then $|arg(\mu_1)| = \pi > \frac{q\pi}{2}$. If $\epsilon\alpha < 1$ then $|arg(\mu_{2,3})| = \pi > \frac{q\pi}{2}\ \forall\ q \in (0,1)$. Following [43,40], the E_4 is locally stable if $\zeta > ax_4 - \frac{b(x_4+\alpha z_4)}{k}$and $\epsilon\alpha < 1$ which implies that the disease will be eliminated in the mice population. □

Finally, the local stability around the coexistence equilibrium point E_5 is investigated as follows. The $J(E_5)$given by

$$J(E_5) = \begin{pmatrix} -\frac{b(x_5^2+ky_5)}{kx_5} & b - \frac{(b+ak)x_5}{k} & -\frac{\alpha bx_5}{k} \\ (a - \frac{b}{k})y_5 & -\frac{by_5}{k} & -\frac{\alpha by_5}{k} \\ -\frac{\epsilon\beta z_5}{k} & -\frac{\epsilon\beta z_5}{k} & -\frac{\beta z_5}{k} \end{pmatrix}. \tag{13}$$

The roots of the following equation are the eigenvalues of (13).

$$V(\mu) = \mu^3 + A_1\mu^2 + A_2\mu + A_3 = 0, \tag{14}$$

where

$$A_1 = \frac{by_5+\beta z_5}{k} + \frac{bx_5}{k} + \frac{by_5}{x_5},$$
$$A_2 = \frac{1}{k^2x_5}\left(ky_5\left(b(b-ak)x_5 + ka^2x_5^2 + b^2y_5\right) + b\beta(ky_5 - (\epsilon\alpha - 1)x_5(x_5 + y_5))z_5\right),$$
$$A_3 = \frac{\beta y_5}{k^2x_5}\left(b(b - ak - b\alpha\epsilon)x_5 + ka^2x_5^2 + b^2(1 - \epsilon\alpha)y_5\right)z_5.$$

Then, the proposition given in [44,45] can be used to determine the stability conditions of E_5.

Now, the proof of the existence of transcritical bifurcation around equilibrium points E_0 $E_1$and $E_2$is given by using Sotomayor's theorem.

Theorem 8 (*Transcritical bifurcation around* E_0). The Hantavirus infection model (4) go through a transcritical bifurcation regarding the bifurcation parameter Haround $E_0(0,0,0)$when $H = H^* = b - c$.

Proof. The Jacobian matrix of the Hantavirus infection model (4) around E_0 with $H = H^* = b - c$ has a zero eigenvalue and takes the following form

$$J(E_0) = \begin{pmatrix} 0 & b & 0 \\ 0 & -\zeta & 0 \\ 0 & 0 & \beta - \gamma \end{pmatrix}. \tag{15}$$

Here, $\mu_1 = \beta - \gamma < 0$ and $\mu_2 = -\zeta < 0$. Let $V = (v_1, v_2, v_3)^T = (v_1, 0, 0)^T$ and $W = (\tau_1, \tau_2, \tau_3)^T = \left(\tau_1, \frac{b}{\zeta}\tau_1, 0\right)^T$ be the two eigenvectors corresponding to the zero eigenvalue of the $J(E_0)$and $(J(E_0))^T$, respectively, where $v_1$and $\tau_1$are any non zero real numbers.

Therefore,

$$W^T(F_H(E_0, H^*)) = 0,$$
$$W^T(DF_H(E_0, H^*)V) = -v_1\tau_1 \neq 0,$$
$$W^T\left(D^2F(E_0, H^*)(V, V)\right) = \left(-\frac{2b}{k}v_1^2 - 2\left(\frac{b}{k} + a\right)v_1v_2 - \frac{2b\alpha}{k}v_1v_3\right)\tau_1 + \frac{b}{\zeta}\left(-\frac{2b}{k}v_2^2 - 2\left(\frac{b}{k} - a\right)v_1v_2 - \frac{2b\alpha}{k}v_2v_3\right)\tau_1 \neq 0.$$

By Sotomayor's theorem for transcritical bifurcation [46], the Hantavirus infection model (4) has a transcritical bifurcation around $E_0$when $H = H^* = b - c$as Hpasses through the value H^*, while no saddle-node bifurcation can occur.

Theorem 9 (*Transcritical bifurcation around* E_1). The Hantavirus infection model (4) go through a transcritical bifurcation regarding the bifurcation parameter Haround $E_1\left(\frac{k(b-\zeta)}{b}, 0, 0\right)$when $H = H_{tr1} = b - c - \frac{b^2}{ak}$ and keeping $\Re_2 < 1$.

Proof. The $J(E_1)$with $H = H_{tr1} = b - c - \frac{b^2}{ak}$ has a zero eigenvalue and takes the following form

$$J(E_1) = \begin{pmatrix} \zeta - b & \zeta + ak\left(\frac{\zeta}{b} - 1\right) & \alpha(\zeta - b) \\ 0 & 0 & 0 \\ 0 & 0 & \frac{\beta\epsilon(\zeta-b)}{b}(1 - \Re_2) \end{pmatrix}. \tag{16}$$

Here, $\mu_1 = \zeta - b < 0$ and $\mu_3 = \frac{\beta\epsilon(\zeta-b)}{b}(1 - \Re_2) < 0$ when $\Re_2 < 1$. Let $V = (v_1, v_2, v_3)^T = \left(v_1, \frac{(\zeta-b)v_1}{\zeta+ak\left(\frac{\zeta}{b}-1\right)}, 0\right)^T$ and $W = (\tau_1, \tau_2, \tau_3)^T = (0, \tau_2, 0)^T$be the two eigenvectors corresponding to the zero eigenvalue of the $J(E_1)$and $(J(E_1))^T$, respectively. Where $v_1$and $\tau_2$are any non zero real numbers.

Therefore,

$$W^T(F_H(E_1, H_{tr1})) = 0,$$
$$W^T(DF_H(E_1, H_{tr1})V) = \frac{-(\zeta-b)v_1\tau_2}{\zeta+ak\left(\frac{\zeta}{b}-1\right)} \neq 0,$$
$$W^T\left(D^2F(E_1, H_{tr1})(V, V)\right) = -\left(\frac{2b}{k}v_2^2 + 2\left(\frac{b}{k} - a\right)v_1v_2 + \frac{2b\alpha}{k}v_2v_3\right)\tau_2 \neq 0.$$

By Sotomayor's theorem [46], the Hantavirus infection model (4) has a transcritical bifurcation around $E_1$when $H = H_{tr1} = b - c - \frac{b^2}{ak}$ which is equivalent to $k = k^* = \frac{b^2}{a(b-\zeta)}$ as $H$and $k$passes through the values $H_{tr1}$and k^*, respectively. While no saddle-node bifurcation can occur.

Theorem 10 (*Transcritical bifurcation around* E_2). The Hantavirus infection model (4) go through a transcritical bifurcation regarding the bifurcation parameter Haround $E_2\left(0, 0, \frac{dk}{\beta}\right)$when $H = H_{tr2} = \frac{b(\beta-d\alpha)}{\beta} - c$.

Proof. The $J(E_2)$with $H = H_{tr2} = \frac{b(\beta-d\alpha)}{\beta} - c$ has a zero eigenvalue $(\mu_2 = 0)$and takes the following form

$$J(E_2) = \begin{pmatrix} 0 & b & 0 \\ 0 & -\frac{bd\alpha+\beta\zeta}{\beta} & 0 \\ -\epsilon d & -\epsilon d & -d \end{pmatrix}. \tag{17}$$

Table 2 Hypothetical parameter values of the fractional-order Hantavirus infection model [10].

Case	a	b	k	c	H	β	γ	α	ϵ	Figure
1	0.1	1	100	0.6	0	1	0.5	–	–	2
2	0.1	1	100	0.6	0	1	0.5	1.5	0.5	3
3	0.1	1	100	0.6	0	1	0.5	0.5	1.5	4
4	0.1	1	100	0.6	0	1	0.5	0.7	0.1	5
5	0.1	1	100	0.6	0	1	0.5	0.3	0.5	6
6	0.1	1	100	0.6	0	1	0.5	1.3	1.3	7, 8
7	0.1	1	–	0.6	–	1	0.5	0.4	0.8	9
8	0.1	1	150	0.6	0.4	1	0.5	0.4	0.8	10
9	0.1	1	15	0.6	0.1	1	0.5	0.4	0.8	11
10	0.1	1	200	0.6	0.1	1	0.5	0.4	0.8	12
11	0.1	1	–	0.6	0	1	0.5	0.4	1.3	13, 14
12	0.1	1	100	0.6	–	1	0.9	0.4	1.3	15, 16

Here, $\mu_1 = -d < 0$ and $\mu_3 = -\frac{bd\alpha+\beta\zeta}{\beta} < 0$. Let $V = (v_1 v_2 v_3)^T = (v_1\ 0\ -\epsilon v_1)^T$ and $W = (\tau_1\tau_2\tau_3)^T = \left(\tau_1\ \frac{b\beta\tau_1}{bd\alpha+\beta\zeta}\ 0\right)^T$ be the two eigenvectors corresponding to the zero eigenvalue of the $J(E_2)$and $(J(E_2))^T$, respectively. Where $v_1$and $\tau_1$are any non zero real numbers.

Therefore,

$$
\begin{aligned}
&W^T(F_H(E_2, H_{tr2})) = 0,\\
&W^T(DF_H(E_2, H_{tr2})V) = -v_1\tau_1 \neq 0,\\
&W^T\left(D^2F(E_2, H_{tr2})(V, V)\right) = \left(-\tfrac{2b}{k}v_1^2 - 2\left(\tfrac{b}{k}+a\right)v_1v_2 - \tfrac{2b\alpha}{k}v_1v_3\right)\tau_1\\
&\qquad + \tfrac{b\beta}{bd\alpha+\beta\zeta}\left(-\tfrac{2b}{k}v_2^2 - 2\left(\tfrac{b}{k}-a\right)v_1v_2 - \tfrac{2b\alpha}{k}v_2v_3\right)\tau_1 \neq 0.
\end{aligned}
$$

By Sotomayor's theorem [46], the Hantavirus infection model (4) has a transcritical bifurcation around $E_2$when $H = H_{tr2} = \frac{b(\beta-d\alpha)}{\beta} - c$ as H passes through the value H_{tr2}. While no saddle-node bifurcation can occur. □

6. Numerical simulations

In this section, the numerical simulations using the numerical method proposed in [47,48] are given to illustrate the properties of the fractional-order Hantavirus model (4) with respect to fractional-order (q), competitive effect of alien species on mice (α), competitive effect of mice on alien species (ϵ), carrying capacity $(k)$and harvesting efforts (H). The basin of attraction regions is also illustrated. The hypothetical parameter values of the model (4) are provided in Table 2 which were also used for the integer-order model [10].

From Fig. 1, it can be observed that the fractional-order is important in that it affects the convergence speed of the solutions of the fractional-order Hantavirus model (4). One can observe that the convergence speed decrease with decreasing the value of fractional-order (q). Fig. 1 also shows that the

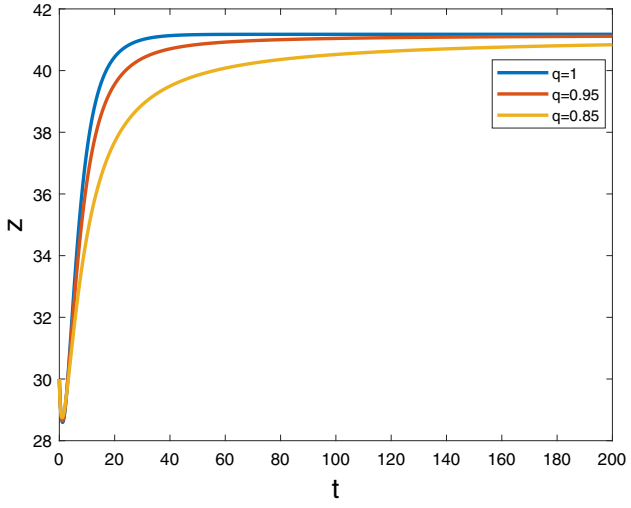

Fig. 1 State trajectories of Hantavirus infection model (4) with different values of fractional.-order (q).

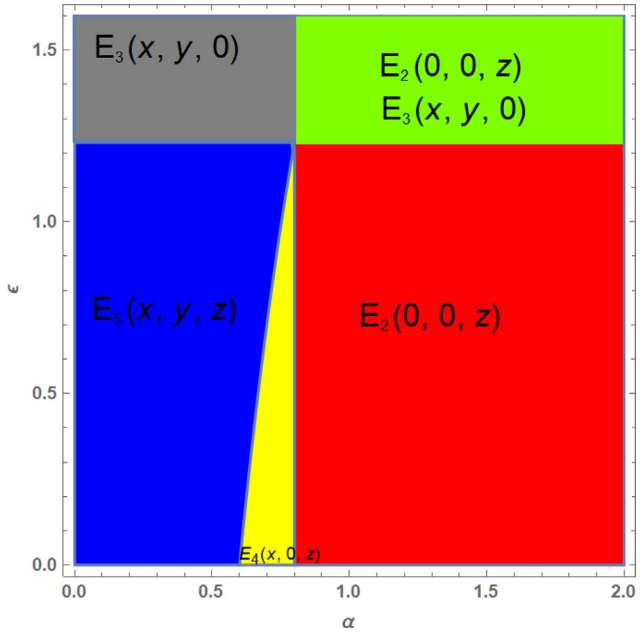

Fig. 2 Local stability regions for the equilibrium points of the fractional-order Hantavirus infection model (4) in (α, ϵ)-plane.

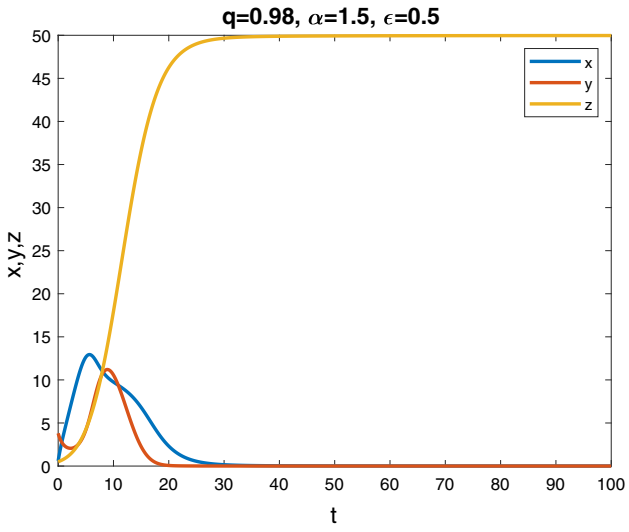

Fig. 3 Local stability of the E_2 when $q = 0.98, \alpha = 1.5$and $\epsilon = 0.5$.

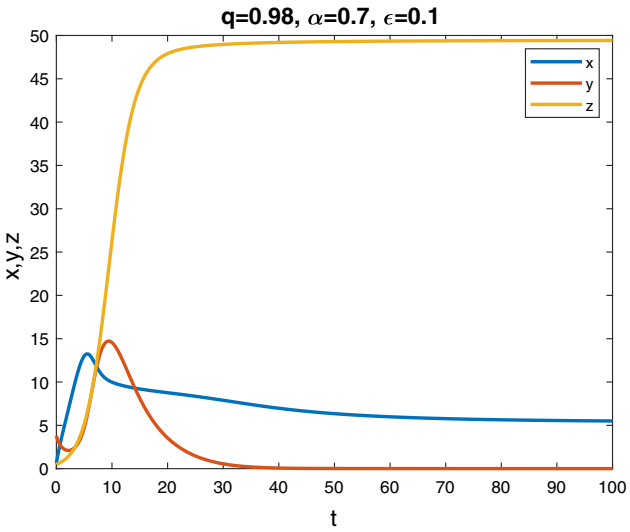

Fig. 5 Local stability of the E_4 when $q = 0.98, \alpha = 0.7$and $\epsilon = 0.1$.

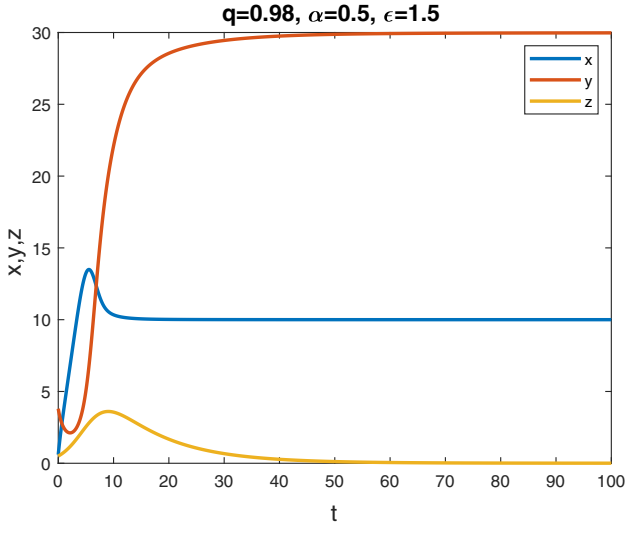

Fig. 4 Local stability of the E_3 when $q = 0.98, \alpha = 0.5$and $\epsilon = 1.5$.

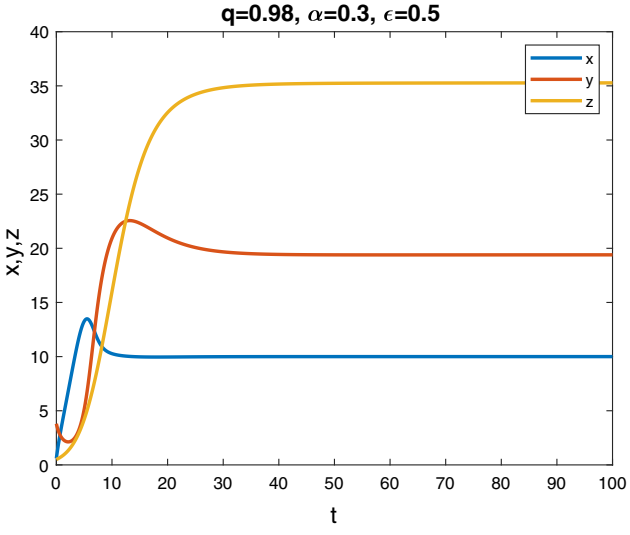

Fig. 6 Local stability of the E_5 when $q = 0.98, \alpha = 0.3$and $\epsilon = 0.5$.

alien species (z) remain stable for different values of fractional-order (q)though solutions reach to $E_5(10, 7.647, 41.176)$ more slowly for a smaller value of fractional-order (q).

Fig. 2 is deduced by the previous local stability theorems which represents the regions of local stability for the E_2, E_3, E_4 and E_5 of the fractional-order Hantavirus infection model (4) in the (α, ϵ)-plane. The region is divided into five different coloured parts: in the red region, $\Re_1 < 1$ which means that the E_2 is locally stable as proved in Theorem 5 and occur with Fig. 3 (when $q = 0.98, \alpha = 1.5$and $\epsilon = 0.5$); the grey region is for local stability of E_3, in this case $\Re_0 > 1$and $\Re_2 < 1$ which coincide with Theorem 6 and concur with Fig. 4 (when $q = 0.98, \alpha = 0.5$and $\epsilon = 1.5$); the yellow region is for local stability of E_4, in this case $\zeta > ax_4 - \frac{b(x_4+\alpha z_4)}{k}$and $\epsilon\alpha < 1$ which coincide with Theorem 7 and concur with Fig. 5 (when $q = 0.98, \alpha = 0.7$and $\epsilon = 0.1$); the blue region is for local stability of E_5 as indicated in Fig. 6 (when $q = 0.98, \alpha = 0.3$and $\epsilon = 0.5$); and the green region shows bistability phenomena for E_3 with initial condition $I_0 = (8, 9, 1)$and E_2 with initial condition $I_0 = (8, 5, 1)$ as shown in Figs. 7(a) and 7(b), respectively (when $q = 0.98, \alpha = 1.3$and $\epsilon = 1.3$).

The basin of attraction regions in the (x_0, y_0)-plane are illustrated in Fig. 8. It is observed that if the initial conditions are chosen from the green region the fractional-order Hantavirus infection model (4) will be closer to the E_3 as indicated in Fig. 8 and coincide with Fig. 7(a) (when $x_0 = 8, y_0 = 9$and $z_0 = 1$); for initial conditions within the red region the model (4) will be closer to the E_2 as shown in Fig. 8 and occur with Fig. 7(b) (when $x_0 = 8, y_0 = 5$and $z_0 = 1$).

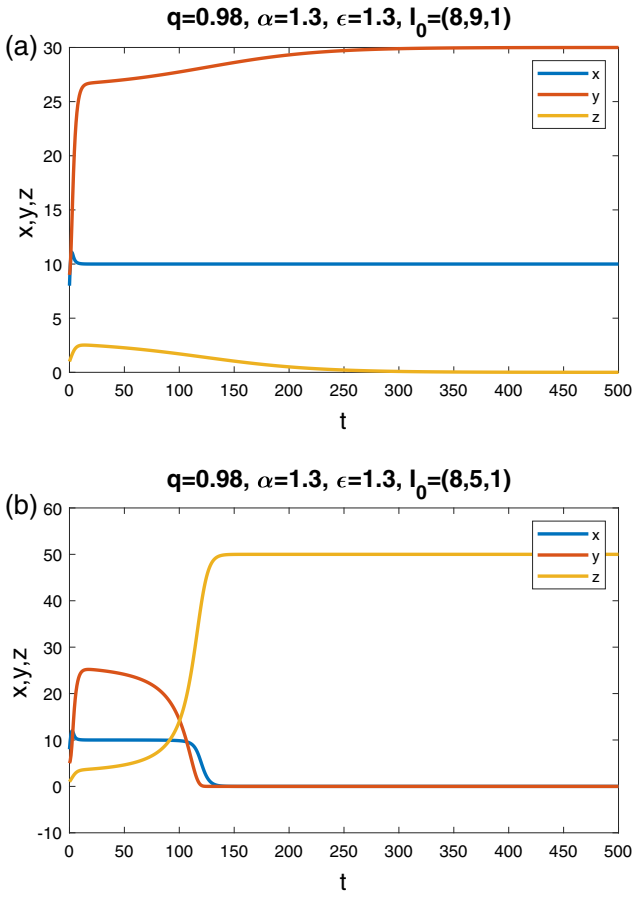

Fig. 7 Local stability of the E_3 and E_2 with different initial conditions and $q = 0.98, \alpha = 1.3$and $\epsilon = 1.3$.

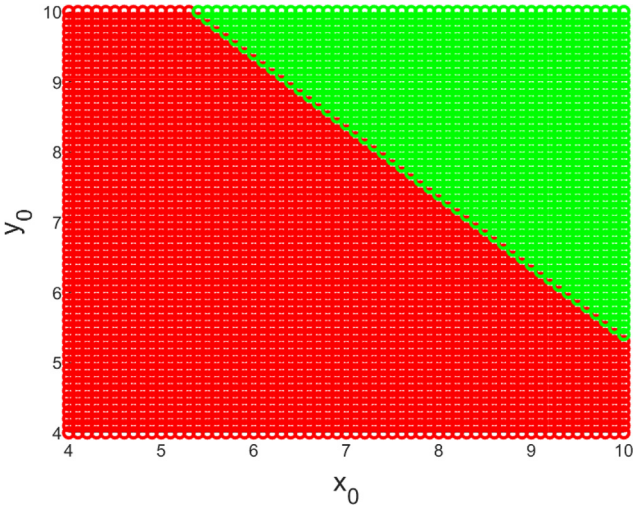

Fig. 8 Basin of attraction in the (initial susceptible mice population (x_0), initial infected mice population (y_0))-plane.

Fig. 9 is deduced by the previous local stability theorems which represents the regions of local stability for the E_2, E_4 and E_5 of model (4) in the (H, k)-plane. The region is divided into three different coloured parts: in the red region, $\Re_1 < 1$

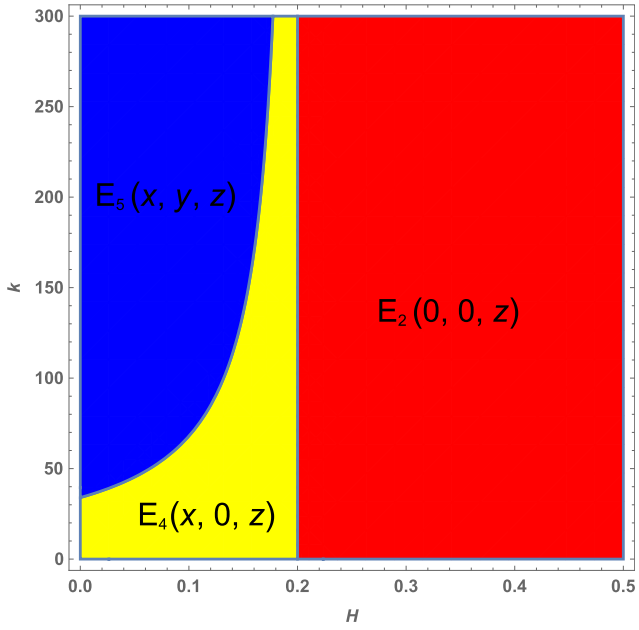

Fig. 9 Local stability regions for the equilibrium points of the fractional-order Hantavirus infection model (4) in $.(H, k)$-plane.

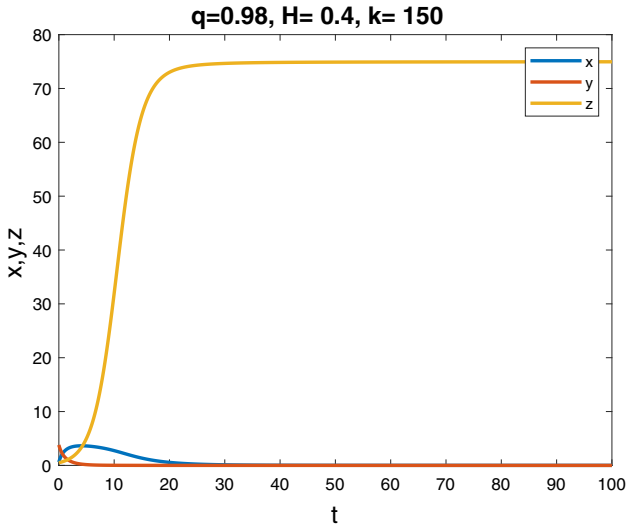

Fig. 10 Local stability of the E_2 when $q = 0.98, H = 0.4$and $k = 150$.

which means that the E_2 is locally stable as proved in Theorem 5 and occur with Fig. 10 (when $q = 0.98, H = 0.4$and $k = 150$); the yellow region is for local stability of E_4, in this case $\zeta > ax_4 - \frac{b(x_4+\alpha z_4)}{k}$and $\epsilon\alpha < 1$ which coincide with Theorem 7 and concur with Fig. 11 (when $q = 0.98, H = 0.1$and $k = 15$); the blue region is for local stability of E_5 as indicated in Fig. 12 (when $q = 0.98, H = 0.1$and $k = 200$).

In order to show the effect of the carrying capacity (k), one can draw the bifurcation diagram with respect to $k$as a bifurcation parameter. It can be observed that the transcritical bifurcation value is centralized at $k^* = \frac{b^2}{a(b-\zeta)} = 25$ which is

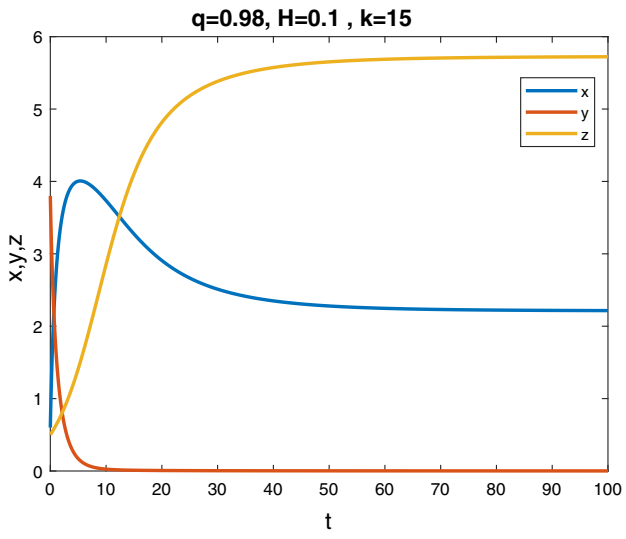

Fig. 11 Local stability of the E_4 when $q = 0.98, H = 0.1$and $k = 15$.

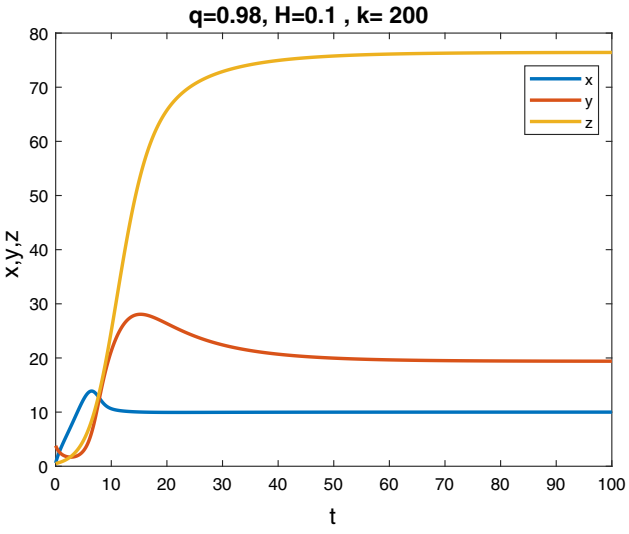

Fig. 12 Local stability of the E_5 when $q = 0.98, H = 0.1$and $k = 200$.

coincide with Theorem 9 and indicated in Fig. 13 (in this case $\Re_2 = 0.961538 < 1$). It can also be observed that when $k < k^*$ the susceptible mice population exist and the infection dies away as indicated in Fig. 13 and coincide with Fig. 14(a) (when $k = 15$). For $k > k^*$ the susceptible and infected mice co-exist and the infection thrives since there is an increase in edible resources as indicated in Fig. 13 and occur with Fig. 14(b) (when $k = 40$). Fig. 14 indicates that both susceptible and infected populations will eventually reach steady states with the values for the susceptible population being higher compared to the infected case.

In order to show the effect of harvesting (H)on the dynamics of the fractional-order model (4), one can draw the bifurcation diagram with respect to H as a bifurcation parameter. It can be observed that the transcritical bifurcation values are centralized at $H_{tr1} = b - c - \frac{b^2}{ak} = 0.3, H_{tr4} = b - c - \frac{bd\alpha}{\beta} +$

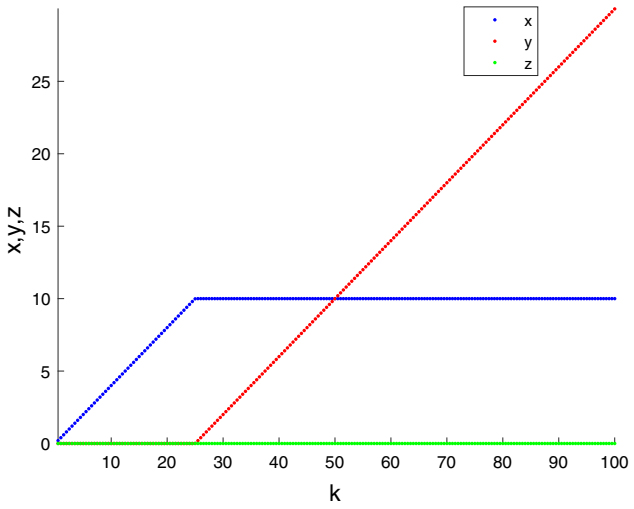

Fig. 13 Bifurcation diagram of the fractional-order Hantavirus infection model (4) regarding carrying ca.pacity (k).

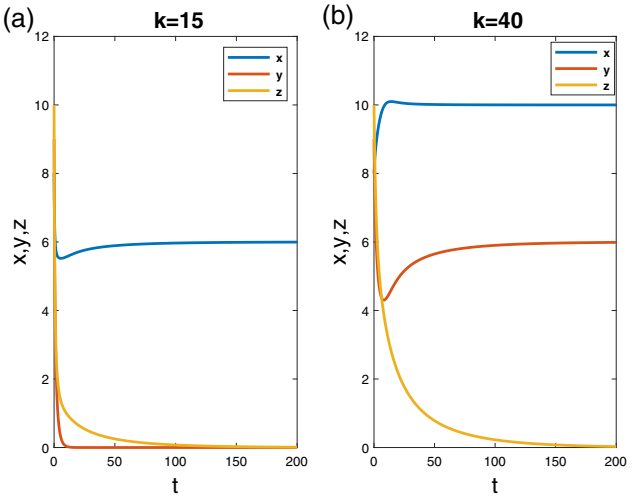

Fig. 14 Time series of the fractional-order Hantavirus infection model (4) with different values of carrying ca.pacity (k).

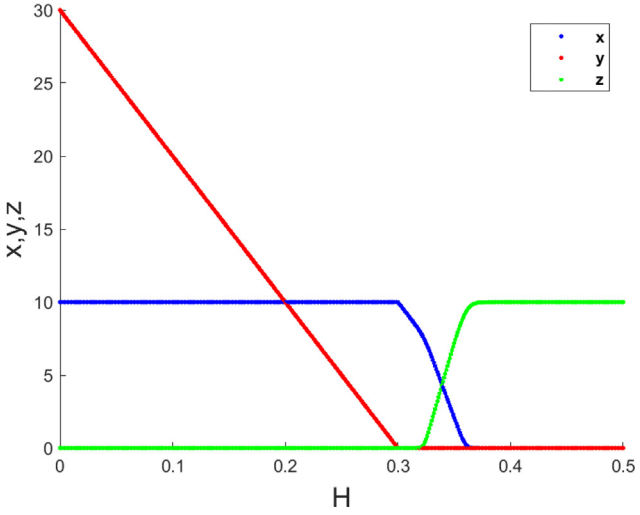

Fig. 15 Bifurcation diagram of the fractional-order Hantavirus infection model (4) regarding harv.esting (H).

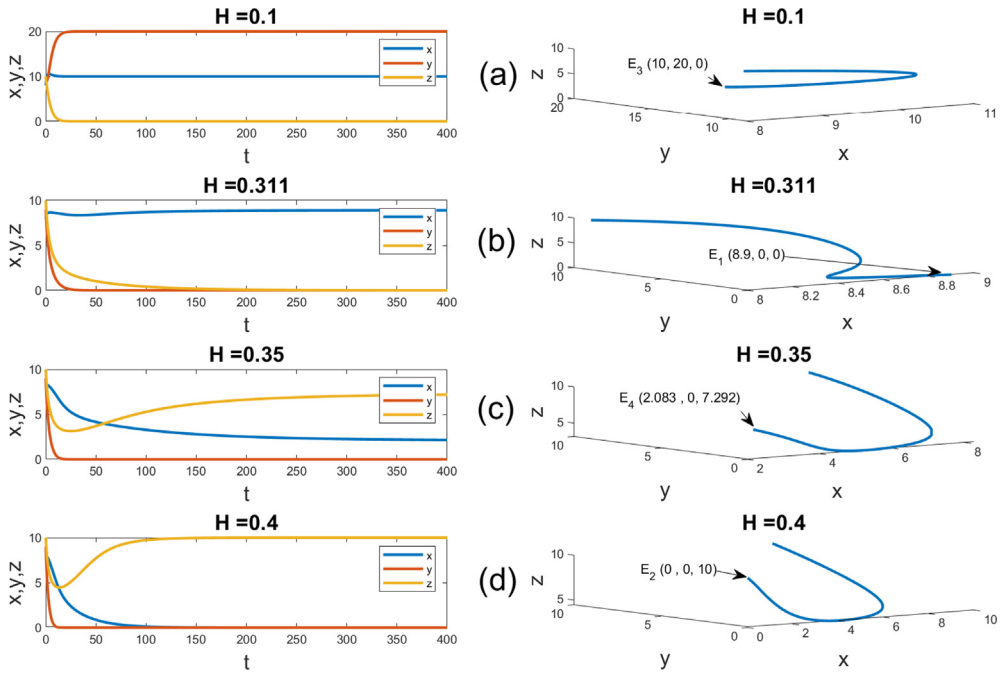

Fig. 16 Time series and phase diagram of the fractional-order Hantavirus infection model (4) with different values of har.vesting (H).

$\frac{b^2(\alpha\epsilon-1)}{ak} = 0.312$and $H_{tr2} = \frac{b(\beta-d\alpha)}{\beta} - c = 0.36$ which is coincide with the theoretical results and indicated in Fig. 15. It can also be observed that when $H < H_{tr1}$ the susceptible and infected mice populations coexist as shown in Fig. 15 and coincide with Fig. 16(a) (when $H = 0.1$). For $H \in (H_{tr1}, H_{tr4})$the susceptible mice population only exist as shown in Fig. 15 and concur with Fig. 16(b) (when $H = 0.311$). For $H \in (H_{tr4}, H_{tr2})$the susceptible mice and alien species coexist and the infection dies away as indicated in Fig. 15 and coincide with Fig. 16(c) (when $H = 0.35$). For $H > H_{tr2}$ the alien species only exist as shown in Fig. 15 and concur with Fig. 16(d) (when $H = 0.4$).

7. Conclusion

A fractional-order Hantavirus infection model incorporating harvesting has been formulated and analyzed in this paper. The fractional-order model describes the spread of Hantavirus infection in a system consisting of populations of susceptible mice, infected mice and alien species. A sufficient condition for the existence and uniqueness of the fractional-order Hantavirus infection model (4) has been obtained. It has been proved that the solution of the fractional order system of differential equations (4) are uniformly bounded and non-negative. The proposed fractional-order Hantavirus infection model has six non-negative equilibrium points. The threshold parameters ($\Re_0$, $\Re_1$, $\Re_2$and$\Re_3$)have been used to determine the existence and stability conditions of the equilibrium points. The local stability of the equilibrium points of the fractional-order Hantavirus infection model (4) has been investigated which can be considered as the main contribution of this paper. The mathematical proof of the existence of transcritical bifurcation has been given by using Sotomayor's theorem. Numerical simulations have been conducted to illustrate the properties of the proposed fractional-order Hantavirus infection model with respect to fractional-order (q), competitive effect of alien species on mice (α), competitive effect of mice on alien species (ϵ), carrying capacity (k)and harvesting efforts (H). The basin of attraction regions has been also illustrated. Future research will focus on the incorporation of time delay in the system and the resulting consequences.

Funding

This work was supported by the Ministry of Higher Education Malaysia and Research Management Centre-UTM, Universiti Teknologi Malaysia (UTM) through the Konsortium Kecemerlangan Pendidikan (KKP) grant with vote number 4L948. Article Processing Charge Funding under Division of Research & Innovation, Universiti Sains Malaysia and Fundamental Research Grant Scheme by Ministry of Higher Education (FRGS/1/2021/STG06/USM/02/09).

Availability of data and material

Not applicable.

Code availability

Not applicable.

Authors' contributions

All authors read and approved the final manuscript.

Declaration of Competing Interest

The authors declare that they have no known competing financial interests or personal relationships that could have appeared to influence the work reported in this paper.

Acknowledgements

The authors would like to acknowledge the Ministry of Higher Education Malaysia and Research Management Centre-UTM, Universiti Teknologi Malaysia (UTM) for financial support. The financial support from Universiti Sains Malaysia for the Article Processing Charge (APC) and FRGS by MOHE are acknowledged.

References

[1] G. Abramson, V.M. Kenkre, Spatiotemporal patterns in the Hantavirus infection, Phys. Rev. E 66 (2002) 011912.
[2] H. Tian, N.C. Stenseth, The ecological dynamics of hantavirus diseases: From environmental variability to disease prevention largely based on data from China, PLoS Neglect. Trop. Diseases 13 (2019) e0006901.
[3] I.D. Peixoto, G. Abramson, The effect of biodiversity on the Hantavirus epizootic, Ecology 87 (2006) 873–879.
[4] M.A. Aguirre, G. Abramson, A.R. Bishop, V.M. Kenkre, Simulations in the mathematical modeling of the spread of the Hantavirus, Phys. Rev. E 66 (2002) 041908.
[5] M. Chen, D.P. Clemence, Analysis of and numerical schemes for a mouse population model in Hantavirus epidemics, J. Diff. Eqs. Appl. 12 (2006) 887–899.
[6] J. Buceta, C. Escudero, F.J. Rubia, K. Lindenberg, Outbreaks of Hantavirus induced by seasonality, Phys. Rev. E 69 (2004) 021906.
[7] G. Abramson, The criticality of the Hantavirus infected phase at Zuni, arXiv preprint q-bio/0407003 (2004).
[8] S.M. Goh, A.I.M. Ismail, M.S.M. Noorani, I. Hashim, Dynamics of the Hantavirus infection through variational iteration method, Nonlinear Anal.: Real World Appl. 10 (2009) 2171–2176.
[9] F.M. Yusof, F.A. Abdullah, A.I. Ismail, Modeling and optimal control on the spread of Hantavirus infection, Mathematics 7 (2019) 1192.
[10] F.M. Yusof, M.H. Mohd, Y.M. Yatim, A.I. Ismail, Effects of biotic interactions, abiotic environments and harvesting on the spread of Hantavirus infection, MATEMATIKA: Malaysian J. Industr. Appl. Math. 36 (2020) 1–14.
[11] A.A. Elsadany, A.E. Matouk, Dynamical behaviors of fractional-order Lotka-Volterra predator–prey model and its discretization, J. Appl. Math. Comput. 49 (2015) 269–283.
[12] A.E. Matouk, A.A. Elsadany, Dynamical analysis, stabilization and discretization of a chaotic fractional-order GLV model, Nonlinear Dyn. 85 (2016) 1597–1612.
[13] M. Sambath, P. Ramesh, K. Balachandran, Asymptotic behavior of the fractional order three species prey–predator model, Int. J. Nonlinear Sci. Numer. Simul. 19 (2018) 721–733.
[14] M. Moustafa, M.H. Mohd, A.I. Ismail, F.A. Abdullah, Dynamical analysis of a fractional-order Rosenzweig-MacArthur model with stage structure incorporating a prey refuge, Prog. Fract. Different. Appl. 5 (2019) 1–17.
[15] H.A. El-Saka, S. Lee, B. Jang, Dynamic analysis of fractional-order predator–prey biological economic system with Holling type II functional response, Nonlinear Dyn. 96 (2019) 407–416.
[16] M. Javidi, B. Ahmad, Dynamic analysis of time fractional order phytoplankton–toxic phytoplankton–zooplankton system, Ecol. Model. 318 (2015) 8–18.
[17] M. Das, G.P. Samanta, A prey-predator fractional order model with fear effect and group defense, Int. J. Dynam. Control (2020) 1–16.
[18] D. Baleanu, F.A. Ghassabzade, J.J. Nieto, A. Jajarmi, On a new and generalized fractional model for a real cholera outbreak, Alexandria Eng. J. 61 (2022) 9175–9186.
[19] A. Jajarmi, D. Baleanu, A new fractional analysis on the interaction of HIV with CD4+ T-cells, Chaos, Solitons & Fractals 113 (2018) 221–229.
[20] F.A. Rihan, Numerical modeling of fractional-order biological systems, in: Abstract and Applied Analysis, Vol. 2013, Hindawi, 2013.
[21] E. Ahmed, A. Hashish, F.A. Rihan, On fractional order cancer model, Journal of Fractional Calculus and Applied, Analysis 3 (2012) 1–6.
[22] F.A. Rihan, A.A. Arafa, R. Rakkiyappan, C. Rajivganthi, Y. Xu, Fractional-order delay differential equations for the dynamics of hepatitis C virus infection with IFN-αtreatment, Alexandria Eng. J. 60 (2021) 4761–4774.
[23] A. Jajarmi, D. Baleanu, K. Zarghami Vahid, S. Mobayen, A general fractional formulation and tracking control for immunogenic tumor dynamics, Mathematical Methods in the Applied Sciences 45 (2022) 667–680.
[24] D. Baleanu, M.H. Abadi, A. Jajarmi, K.Z. Vahid, J.J. Nieto, A new comparative study on the general fractional model of COVID-19 with isolation and quarantine effects, Alexandria Engineering Journal 61 (2022) 4779–4791.
[25] M. Moustafa, M.H. Mohd, A.I. Ismail, F.A. Abdullah, Dynamical analysis of a fractional-order Hantavirus infection model, International Journal of Nonlinear Sciences and Numerical Simulation (2019).
[26] S.Z. Rida, A.S. Abd-elradi, A. Arafa, M. Khalil, The effect of the environmental parameter on the Hantavirus infection through a fractional-order SI model, International Journal of Basic and Applied Sciences 1 (2012) 88–99.
[27] F.A. Abdullah, A.I. Ismail, Simulations of the spread of the Hantavirus using fractional differential equations, Matematika 27 (2011) 149–158.
[28] F.A. Rihan, Q.M. Al-Mdallal, H.J. AlSakaji, A. Hashish, A fractional-order epidemic model with time-delay and nonlinear incidence rate, Chaos, Solitons & Fractals 126 (2019) 97–105.
[29] M. Moustafa, M.H. Mohd, A.I. Ismail, F.A. Abdullah, Dynamical analysis of a fractional order eco-epidemiological model with nonlinear incidence rate and prey refuge, Journal of Applied Mathematics and Computing (2020) 1–28.
[30] M. Moustafa, M.H. Mohd, A.I. Ismail, F.A. Abdullah, Dynamical analysis of a fractional-order eco-epidemiological model with disease in prey population, Advances in Difference Equations 2020 (2020) 48.
[31] M. Danca, Hidden chaotic attractors in fractional-order systems, Nonlinear Dyn. 89 (2017) 577–586.
[32] J. Alidousti, M. Ghahfarokhi, Dynamical behavior of a fractional three-species food chain model, Nonlinear Dyn. (2018) 1–18.
[33] B. Ghanbari, S. Djilali, Mathematical analysis of a fractional-order predator-prey model with prey social behavior and infection developed in predator population, Chaos, Solitons & Fractals 138 (2020) 109960.
[34] M.A. Khan, S. Ullah, M. Farhan, Fractional order SEIR model with generalized incidence rate, AIMS Mathematics 5 (2020) 2843.
[35] Y. Yang, L. Xu, Stability of a fractional order SEIR model with general incidence, Applied Mathematics Letters 105 (2020) 106303.
[36] R. Almeida, B. Cruz, N. Martins, T. Monteiro, An epidemiological MSEIR model described by the Caputo fractional derivative, International Journal of Dynamics and Control (2018) 1–9.

[37] A.A. Kilbas, H.M. Srivastava, J.J. Trujillo, Theory and Applications of Fractional Differential Equations, Elsevier, Amsterdam, 2006.
[38] M. Das, A. Maiti, G.P. Samanta, Stability analysis of a prey-predator fractional order model incorporating prey refuge, Ecological Genetics and Genomics 7 (2018) 33–46.
[39] C.P. Li, F.R. Zhang, A survey on the stability of fractional differential equations, The European Physical Journal-Special Topics 193 (2011) 27–47.
[40] I. Petras, Fractional-order Nonlinear Systems: Modeling, Analysis and Simulation, Springer Science and Business Media, 2011.
[41] J. Cresson, A. Szafrańska, Discrete and continuous fractional persistence problems–the positivity property and applications, Commun. Nonlinear Sci. Numer. Simul. 44 (2017) 424–448.
[42] S.K. Choi, B. Kang, N. Koo, Stability for Caputo fractional differential systems, Abstract and Applied Analysis 2014 (2014) 1–6.
[43] E. Ahmed, A. El-Sayed, H.A. El-Saka, Equilibrium points, stability and numerical solutions of fractional-order predator–prey and rabies models, Journal of Mathematical Analysis and Applications 325 (2007) 542–553.
[44] A.E. Matouk, Chaos, feedback control and synchronization of a fractional-order modified Autonomous Van der Pol-Duffing circuit, Commun. Nonlinear Sci. Numer. Simul. 16 (2011) 975–986.
[45] M.S. Abdelouahab, N. Hamri, J. Wang, Hopf bifurcation and chaos in fractional-order modified hybrid optical system, Nonlinear Dyn. 69 (2012) 275–284.
[46] J. Guckenheimer, P. Holmes, Nonlinear oscillations, dynamical systems, and bifurcations of vector fields, Vol. 42, Springer Science & Business Media, 2013.
[47] K. Diethelm, N.J. Ford, A.D. Freed, A predictor-corrector approach for the numerical solution of fractional differential equations, Nonlinear Dyn. 29 (2002) 3–22.
[48] C. Li, C. Tao, On the fractional Adams method, Comput. Math. Appl. 58 (2009) 1573–1588.